

Deployment of active Thomson spectrometer at Vulcan petawatt

Contact: daniel.bedilu@stfc.ac.uk

D. Bedilu

*Experimental Science Group,
Central Laser Facility, RAL,
OX11 0QX, United Kingdom*

D.C. Carroll

*Experimental Science Group,
Central Laser Facility, RAL,
OX11 0QX, United Kingdom*

Abstract

Three different scintillators were tested in an real-time Thomson parabola spectrometer, capable of high (10Hz) rep rate acquisitions. The scintillators tested were a Cerium doped Lutetium (LYSO) crystal, a terbium-doped gadolinium oxysulphide ceramic phosphor (Gadox:Tb), and a commercially available Lanex medium scintillator, also utilising Tb doped Gadox. Each of these were tested and measured against Fujifilm image plate, which is commonly used for ion detection in Thomson spectrometers. It is found that the ceramic phosphor has the highest sensitivity of the scintillators used and is capable of measuring signal using a $410\mu\text{m}$ pinhole. However this sensitivity is still about 20 times lower than conventional image plate.

1 Introduction

The Thomson parabola spectrometer (TPS) is a commonly used diagnostic for measuring the energy of ions. The ions pass through a pinhole then are spread out in energy using magnets and also spread orthogonally by mass to charge ratio using a pair of electrically charged plates. The ions are then detected using a detector such as image plate, CR39 or a microchannel plate (MCP), which can then be read to produce a spectrum from the parabolas produced. The problem with these detectors is that they require a lot of time to read; on the scale of tens of minutes to scan a piece of image plate, and up to several hours to etch and then read a piece of CR39. For high power laser experiments, this involves letting the chamber up in order to retrieve the detector. With the ongoing development of high power - high rep rate lasers such as the upcoming Extreme Photonics Application Center (EPAC) [1], these traditional detectors become infeasible with their long read times and single-use nature. The use of scintillators as detectors allows for immediate, on shot imaging of the ion spectra. Previous work has been done on developing an active TPS diagnostic with scintillators as particle detectors [2]. This work explores the possibility of different scin-

H. Ahmed

*Experimental Science Group,
Central Laser Facility, RAL,
OX11 0QX, United Kingdom*

R.J. Clarke

*Experimental Science Group,
Central Laser Facility, RAL,
OX11 0QX, United Kingdom*

tillators for use as detectors as well as the applicability at much higher energies than previously tested.

2 Method

The use of scintillators as detectors allows for the immediate detection of the spectra by using a camera to image the scintillation, done here using an Andor Neo scientific CMOS (sCMOS). A sCMOS was used over an EMCCD partially due to availability reasons, as sCMOS cameras are more readily available. An existing TPS design [3]

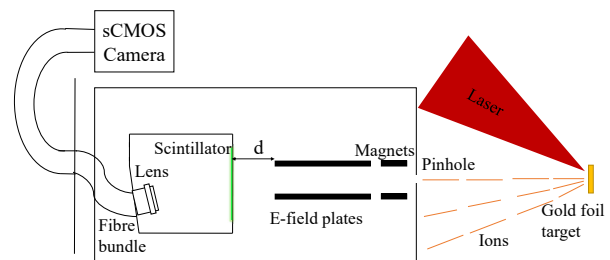


Figure 1: Diagram of the real-time Thomson spectrometer setup.

was modified in order to achieve real time functionality. A scintillator housing was placed on the rail that usually holds a stand for image plate. The setup as shown above involves a housing used to hold the scintillator, as well as a Navitar 25mm f0.95 lens. Directly behind the lens a 8mm by 8mm fibre bundle is screwed in with fibre size of $10\mu\text{m}$. The bundle exits the chamber through a vacuum feedthrough tube. The other end of the fibre bundle screws onto a windowed flange with a Hamamatsu 1:1 relay lens connected to the other side of the flange which is then connected to the Andor Neo camera. The entire imaging system was tested using a standard 1951 USAF resolution test chart, being able to resolve to group 2 element 1, corresponding to a resolution of $125\mu\text{m}$. Testing was also done on the variance of resolution across the surface of the phosphor, which was found not to be of significance. These tests were done on the

whole system including the fibre bundle, lens and camera. Given that the only real difference from a standard TPS is the detector setup, the detector assembly used here is very easy to attach onto existing TPS designs to enable real-time functionality. The use of the housing for the scintillator allows for improved light tightening, which is of great concern to image quality. The strength of the magnetic field was measured using a hall probe. The magnetic dispersion was confirmed by using a piece of $500\mu\text{m}$ thick iron in front of a piece of image plate it was calculated using SRIM[4], that only protons above 14.65MeV would pass through and be seen on the image plate. Using this and the equation for deflection of ions by magnets in a TPS [3], the strength of the magnets was calculated to be 0.96T . The electrodes were set to their maximum potential difference they could handle on each shot, this is theoretically 25kV , however this was only achieved consistently during the latter half of tests, and actual potential difference was lower, varying during the first half of tests. The field of view was limited by the physical size of the fibre bundle at 4.7m by 4.7cm . Using this information and the dispersion equation for Thomson spectrometers, the minimum theoretical proton energy visible to this system is 3.99MeV . This is calculated with the distance 'd' (fig.1) at 110mm . The scintillators used were a ceramic gadox based phosphor, with an active layer μm thick. Two thicknesses of LYSO were tested, $500\mu\text{m}$ and 2mm . The ceramic phosphor also includes a reflective backing, theoretically doubling its light output. As for lanex, being a commercial product means there is little available information on its construction. An ion beam was produced using Vulcan's petawatt beam on interaction with a $10\mu\text{m}$ gold foil. Laser energies varied between 311J and 366J shot to shot. The angle of incidence of the laser on the foil was 15° (??)

3 Results

On each shot the camera was set to trigger 50ms before the shot with an exposure time of 100ms , theoretically allowing 10Hz operation, however due to the limited repetition rate on Vulcan of about 1 shot every 20 minutes, this was not tested. Initially a pinhole of 1mm diameter was used and distance 'd' was set to 197mm . The spectrometer was placed along the front surface, close to target normal. The front surface is irradiated by the Vulcan beam, producing high energy ions through target normal sheath acceleration.

The main figure of merit for each image was taken as the signal to noise ratio. Signal to noise ratio was measured by taking the brightness of the proton trail at 15MeV as representative on each scintillator. Unfortunately, due to the position of the setup changing slightly between scintillators, it was not possible to do an exact pixel to pixel comparison to compare signal strengths. Noise was measured as the standard deviation of the

background of the image.

Initial testing with Gadox resulted in good spectra being seen, however there was a clear banding structure in the background of the image which was bright compared to the ion signal. This bright background resulted in a low signal to noise ratio. Efforts were taken to reduce the bright background signal. Due to the fibre being loose and unshielded in the chamber, it was hypothesised that part of the problem could be x-ray induced scintillation within the fibre. An image was taken during a shot with the lens imaging the scintillator capped; the same background pattern was still observed, supporting the earlier hypothesis. To alleviate this, lead sheets were wrapped around the fibre bundle. Due to practical considerations, it was not possible to shield the entire length of the fibre in the chamber using lead sheeting. For the remaining length of fibre black aluminium foil was wrapped around it, and then a rubber hose wrapped again around that. With these measures the background noise was again reduced further. The improved background noise can be seen in Fig.2 where the average background signal was reduced from 2488 counts to 555 counts, a 4.5 times decrease in background noise. Similar reduction in background noise was also seen for the other scintillators. The glow time of each of the scintillators was checked



Figure 2: Images from lanex, before shielding (left) and after full shielding (right).

to see if afterglow would be an issue. The glow time for gadox is 1ms [5] and 45ns for LYSO [6]. For LYSO this is defined as the time it takes for the intensity of scintillation to reach $1/e$ of its peak after an initial excitation. For gadox it is defined as the time for brightness to go reach 10% of its peak from 90% of its peak. Given these times are small compared to the 100ms exposure of the camera, it was determined that scintillator glow would not be of relevance to the testing of these scintillators.

Due to LYSO being transparent, unlike Lanex or the ceramic gadox scintillator, the light tightness of the setup was severely diminished. To alleviate this a piece of $16\mu\text{m}$ thick household aluminium foil was placed in front of the LYSO to block light. Using SRIM[4] it was calculated this would only stop protons up to 1.1MeV , which is

outside the range of ions visible on the system, so it was found to be of no concern. Average background reading was reduced by a factor of 3.8. All testing with LYSO hereafter included this aluminium filter.

To also increase the signal from LYSO, the 1mm pinhole was used for all tests, and the detector setup was moved closer to the electric field plates with $d=20\text{mm}$ in order to try and maximise flux. By moving the scintillator closer to the electric field plates, the horizontal spread of ions at the scintillator is reduced, increasing local brightness due to more overlapping of ion species. Using this setup a signal was visible both on 2mm thick LYSO and 0.5mm thick LYSO.

A 410um pinhole was also tested. The current limiting factor for precision of this system is pinhole size. By differentiating the equation for the magnetic spread of ions with respect to energy, we find that dE/dy is inversely proportional to y^3 and so this decrease in pinhole size increases precision in energy by a factor of 14.5. With a smaller pinhole size it also becomes easier to discern between different ion species and charge states. With the smaller pinhole size, to offset the lower flux, the distance 'd' was reduced to 110mm from the initial 197mm.

Calibration of the ceramic gadox to image plate was done by placing a piece of image plate with regularly spaced slots in front of the scintillator in order to get a like for like comparison of the two. Due to shot to shot variation in laser energy, it was not possible to simply take an image of image plate and then one of a scintillator to compare the two. By looking at parts of the spectra near the edges of the slits on each material a like for like comparison can be made assuming minimal difference in flux between the signal over the edge of a slit between image plate and the scintillator. It was found that image plate has an average SNR of 522 measured at 15MeV, with the scan taken 1 hour and 7 minutes after the shot, compared to the ceramic gadox with a SNR of 26. Using this method it is also possible to convert counts to protons on gadox given that Image plate has previously been well calibrated [5][6]. We find that the conversion factor is 1720 counts per proton at 30 minutes time of scanning. Using the best signal to noise ratio for gadox that was calculated and using a conservative estimate that a minimum SNR of about 2.8 is needed for a discernible signal, we find that the minimum flux that can be detected by gadox is 16 protons/ $25\mu\text{m}^2$. Doing the same comparison with Lanex, we find the minimum flux detectable is 18 protons/ $25\mu\text{m}^2$.

One possible reason for the efficacy of both of the gadox based scintillators over LYSO may be because of the difference in spectra produced by each. Gadox has a peak emission wavelength of 545nm [7] and LYSO of 410nm [8]. Cross referencing this with the quantum efficiency curve of the Neo camera used in this experiment [9], we find the quantum efficiency for gadox to be 55% and 34% for LYSO. Of course, inherent differences in

Scintillator comparison			
Detector	Pinhole size(μm)	Distance 'd'(mm)	SNR
Lanex	1000	197	21.7
Lanex	410	1910	24.3
Lyso 500 μm m	1000	20	11.7
LYSO 2mm	1000	20	11.5
Ceramic gadox	410	110	26
Image plate	410	110	522

Figure 3: Table of SNR values for the different scintillators tested. All values are from after the improved shielding was added.

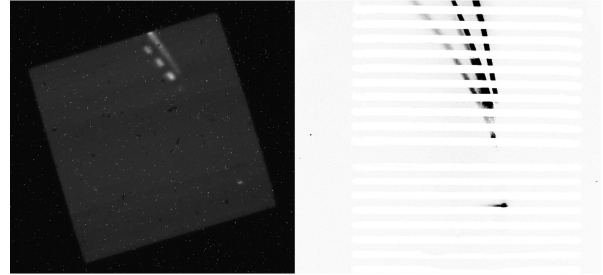


Figure 4: Images from the slotted image plate (left) calibration with ceramic gadox (right).



Figure 5: Best comparison between gadox(left) and lanex(right).

brightness are also likely to play a role.

4 Conclusion

In conclusion, it has been found that in terms of brightness, ceramic gadox phosphor has found to be better than 2mm and 500um thick LYSO as well as Lanex sheets. However, its brightness and signal to noise ratio are still much lower than the current standard of image plate. This raises concerns about applicability in lower flux environments than the ones achieved with Vulcan. Accuracy of actual ion count is lower compared to CR39

where individual pits can be counted, however due to the comparison with calibrated image plate, ion count can be reasonably ascertained. High rep rate applicability, up to 10Hz, is theoretically shown by the use of a 100ms exposure. Testing on a high rep rate laser system will have to be done to experimentally demonstrate this, but due to the low glow time of all the scintillators used, there should theoretically be no issue. Lower background noise may be achievable using a more thorough or even application of shielding for the fibre optic bundle.

One concern for future use of these scintillators for high energy high rep rate applications is their durability over time. Given that the main application of the scintillators used here has historically been in x-ray detection, the understanding of ion damage on these materials is underexplored for determining suitability for long term use. X-ray damage to gadox has been studied [source?], however this is likely a minor issue due to the pinhole blocking most xrays - leaving only the zero point on the scintillator susceptible to x-ray degradation.

A possible improvement to the sensitivity could be achieved through the use of an EMCCD camera rather than a sCMOS. The increased sensitivity would also allow for a reduced pinhole size, increasing precision in energy.

Due to the short glow times of the phosphors used, the necessity of a 100ms exposure is questioned. The time of flight from the target to the scintillator would be 23.5ns for a 30Mev proton and 276ns for a 2.5Mev carbon ion. The ions are produced and accelerated in the laser plasma interaction on the scale of femtoseconds. Given this, it is shown that a more appropriate exposure time would be 2 milliseconds. The andor neo has an internal maximum acquisition start delay of 1 frame [10], so at 100fps operation this enables triggering the camera only a couple of milliseconds before shot. This would drastically reduce background noise from light leakage.

By taking an image not on shot with the same camera parameters light leakage has been found to account for about 300 counts of noise. Assuming linearity with exposure time, an exposure of 2ms would reduce light leakage related background noise to 6 counts.

References

- [1] Danson, C., White, M., Barr, J., Bett, T., Blyth, P., Bowley, D., . . . Winstone, T. (2021). A history of high-power laser research and development in the United Kingdom. *High Power Laser Science and Engineering*, 9, E18. doi:10.1017/hpl.2021.5
- [2] Xu et al, 2011 *Chinese Phys. Lett.* 28 095203 (2011) doi: 10.1088/0256-307x/28/9/095203
- [3] D. Gwynne, S. Kar, D. Doria, H. Ahmed, M. Cerchez, J. Fernandez, R. J. Gray, J. S. Green, F. Hanton, D. A. MacLellan, P. McKenna, Z. Najmudin, D. Neely, J. A. Ruiz, A. Schiavi, M. Streeter, M. Swantusch, O. Willi, M. Zepf, and M. Borghesi, "Modified Thomson spectrometer design for high energy, multi-species ion sources", *Review of Scientific Instruments* 85, 033304 (2014) <https://doi.org/10.1063/1.4866021>
- [4] J.F. Ziegler, M. Ziegler and J. Biersack, SRIM — the stopping and range of ions in matter (2010), *Nucl. Instrum. Meth. B* 268 (2010) 1818 doi:10.1016/j.nimb.2010.02.091.
- [5] Doria et al *Review of Scientific Instruments* 82, 073301 (2011); <https://doi.org/10.1063/1.3606446>
- [6] Alejo et al *Review of Scientific Instruments* 85, 093303 (2014); <https://doi.org/10.1063/1.4893780>
- [7] ProxiVision, "PV Phosphor Screens", https://www.proxivision.de/wp-content/uploads/PV_Phosphor_Screens_201601.pdf, (2016)
- [8] Saint-Gobain, "LYSO material data sheet", <https://www.crystals.saint-gobain.com/sites/imdf.crystals.com/files/documents/lyso-material-data-sheet.pdf>, (2018)
- [9] Andor Oxford instruments, "Andor Neo sCMOS specifications", <https://andor.oxinst.com/assets/uploads/products/andor/documents/andor-neo-scmos-specifications.pdf>
- [10] Andor Oxford instruments, "Andor Neo sCMOS hardware guide", https://andor.oxinst.com/downloads/uploads/Neo_sCMOS_Hardware_Guide.pdf